PHYSICAL REVIEW B VOLUME 28, NUMBER 6 15 SEPTEMBER 1983

High-pressure optical absorption and x-ray-diffraction studies in RbI and KI approaching the metallization transition

K. Asaumi, T. Suzuki, and T. Mori
Institute for Solid State Physics, The University of Tokyo, Roppongi, Minato-ku,
Tokyo 106, Japan
(Received 22 February 1983)

The pressure dependence of the fundamental optical absorption edges in RbI and KI crystals has been investigated up to 70 GPa at room temperature by using high-pressure apparatus of sapphire and diamond anvil types. The absorption edges in RbI and KI are found to show some complicated behaviors below ~5 GPa within the uv region. Beyond ~5 GPa, absorption edges decrease monotonically with increasing pressure up to 70 GPa. The x-ray-diffraction study shows that the CsCl-type crystal structure remains stable up to 67 GPa after the NaCl- to CsCl-type phase transition at 0.4 GPa for RbI and at 1.9 GPa for KI, respectively. The metallization pressures of RbI and KI are estimated to be approximately 85 and 115 GPa, respectively.

I. INTRODUCTION

The pressure-induced insulator-to-metal transition in some systems is one of the most interesting phenomena in high-pressure physics. Band theory predicts that any insulator becomes metallic under extremely high pressure; the valence and conduction bands overlap. Metallic hydrogen, for example, has attracted much attention during the last decade because of its simple electronic configuration and its interests in planetary science. Many authors calculated the metallic transition pressure of solid hydrogen as occurring at several Mbar (100 GPa). No experimental result generally accepted has, however, been obtained.[1]

Although metallic hydrogen as yet remains in the realm of speculation, we think that it is a good time to investigate the pressure-induced metallization of some simple materials since the pressure of near Mbar can be obtained by diamond-anvil cell. From the experimental point of view, the heavy materials have more advantages than the light materials such as the solid hydrogen and LiH,[2] because the heavy materials have generally larger initial compressibility than the light ones when the crystal-structure and chemical-bond character are the same. Our major interest has been centered on the pressure-induced insulator-to-metal transition in some simple electronic and crystal-structural systems such as the alkali halides[3] and solid rare gases.[4] Especially for CsI the metallization pressure has been estimated to be approximately 70 GPa (Ref. 3) which is now within attainable pressure range using a diamond-anvil apparatus. Besides investigating the metallization in CsI, it is necessary to perform the high-pressure optical absorption measurements of other alkali halides to obtain the systematic knowledge of the band-gap behaviors and to obtain their metallization pressures. This is the motive force of this paper.

Eby *et al.*[5] and later Teegarden and Baldini[6] showed that the band-gap energies (E_g) of alkali halides at 0 GPa depend mainly on the halogen ions: $E_g \sim 9$, 7, and 6 eV for alkali chlorides, alkali bromides, and alkali iodides, respectively. On the other hand, high-pressure x-ray-diffraction studies revealed that RbX and KX (X = Cl, Br, and I) undergo a structural phase transition from NaCl- ($B1$-) to CsCl- ($B2$) type structure at about 0.4 and 2.0 GPa, respectively.[7] Thus the pressures of the $B1$-$B2$-type transition depend mainly on alkali ions. Although a number of x-ray studies are reported on these $B1$-$B2$ phase transitions in RbX and KX, further x-ray diffraction study on the crystal-structure problem and pressure-volume relation at very high pressure has not yet been investigated.

This paper deals with the effect of high pressure on the optical absorption edges in RbI and KI with the aim at metallization. Sapphire anvils, type-II a, and type-I diamond anvils were used to obtain the absorption-edge energies at high pressures. Since these materials are reported to exhibit $B1$-$B2$ phase transition at 0.4 (RbI) and 1.9 GPa (KI) with the distinct decrease of volume by about 10%, investigation of the absorption edges before and after this $B1$-$B2$ transition is the first purpose of this study. The x-ray diffraction study of RbI and KI has been performed up to 67 GPa using a diamond-anvil cell in order to confirm the crystal structure at around half Mbar region and to obtain the equations of state. This is the second purpose. Finally, the possible metallic transition of RbI and KI at Mbar (100 GPa) region is discussed.

II. EXPERIMENTAL

A cutaway cross-section drawing of the diamond (and also for sapphire) anvil cell used in the present optical absorption study is illustrated in Fig. 1. The most important mechanisms in a diamond-anvil cell are to adjust the positions of the two anvil faces correctly and to keep the two anvil faces completely parallel even at very high pressure. The position adjustment was made by shifting the lower diamond-mount plate along x-y directions with the small screws. A simple cone and spherical-surface combination is devised for the parallel adjustment of the two anvil faces in this apparatus. A parallel adjustment was performed only by fixing the three screws firmly while ob-

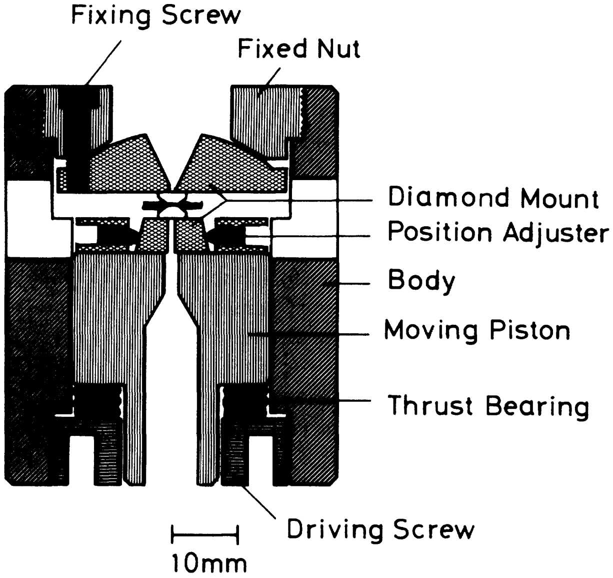

FIG. 1. Cut-away cross-section drawing of the high-pressure diamond cell used in the present optical absorption measurements. The essential components include diamond mounts, position adjusters, a moving piston, thrust bearings, and a driving screw. The parallel adjustment of two anvil faces are performed by a relative movement of the cone (fixed nut) and spherical surface (upper diamond mount). Pressures of above 50 GPa are generated regularly with this apparatus.

serving optical interference patterns to erase between the two anvil faces. This cone and spherical-surface combination mechanism guarantees the parallel feature of two anvil faces up to very high pressures. Pressures of above 50 GPa are regularly generated with this apparatus. Three types of anvils were adopted in the present optical absorption study: sapphire anvils between the photon energy 4 and 6 eV, type-II a diamond anvils between the photon energy 3 and 5.5 eV, and type-I diamond anvils below the photon energy 4 eV. Transmission spectra of these two types of diamonds from uv to visible region are already reported in our previous paper.[3] The experimental setup adopted in the present optical absorption measurement is also reported in Ref. 3. Light sources were a D_2 lamp for the uv region and an I_2 lamp for the visible and near ir region. A prism monochromator of suprasil and/or flint glass was used. Light detectors were a photomultiplier (Hamamatsu R 955) above the photon energy 1.4 eV and a PbS detector below the photon energy 1.5 eV. Both of them were used in combination with a light chopper (400 Hz) and a lock-in amplifier.

Single crystals of RbI and KI were obtained from Harshaw Chemical Company. The sampling procedure was as follows. A metal gasket of 200 μm thick was precompressed by the diamond anvils to ~ 100 μm thick, and a hole of 60 μmϕ was drilled just at the center of the precompressed gasket. A few fragments of ruby particles of about 10 to 20 μm diameter were adhered to the center of the upper diamond anvil face. Single crystals of RbI and KI were cleaved to about 200 μm thick and loaded within the gasket hole by pressing down the moving piston firmly. The excess sample protruded from the gasket hole and was cleaned off completely. X-ray diffraction patterns were obtained by using a lever-arm-type diamond cell similar to that developed by Mao and Bell.[8] X-ray beams generated by a high-power (55 kV—160 mA) rotating anode Mo target were focused onto the sample using a 100 μmϕ pinhole collimator with Zr filter. Diffraction patterns were recorded on the photographic films with the typical exposure time of two hours. Pressures were calibrated by the ruby $R\,1$ fluorescence scale.[9,10] Pressure distribution remained within $\pm 3\%$. All measurements were performed at room temperature.

III. RESULTS

Typical optical-density curves of RbI up to 69 GPa and those of KI up to 71 GPa are shown in Figs. 2 and 3, respectively. For both materials the optical-density curves initially shifted to the high-energy side (blue shift) with increasing pressure. The optical-density curve of KI at 1.9 GPa lies in the high-energy side of that of 0 GPa. This is also true for RbI but the amount of shift is small since $B\,1$-$B\,2$ phase transition occurs at a relatively low pressure 0.4 GPa. The optical-density curve of RbI at 0.4 GPa is abbreviated to avoid the complexity of Fig. 2. Above ~ 5 GPa optical-density curves of RbI and KI shifted monotonically to the low-energy side (red shift). The absorption curves of RbI crossed over the visible region (3.1 to 1.8 eV) from about 35 GPa, so the sample showed continuous change in color from light yellow (~ 35 GPa) to dark red (~ 65 GPa). At 69 GPa, RbI was completely opaque. The coloration of KI was also observed from about 40 GPa. In this case, however, KI was still orange at 71

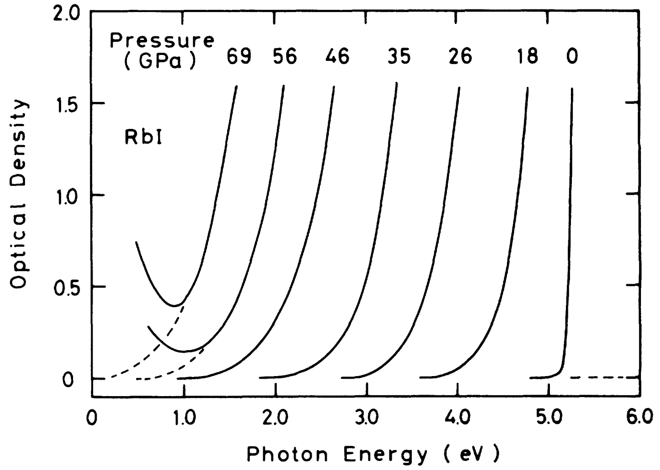

FIG. 2. Typical optical-density curves of RbI at various high pressures. Above 35 GPa the absorption edge crosses over the visible region (from 3.1 to 1.8 eV), so that the sample shows the continuous change in color from light yellow (~ 35 GPa) to dark red (~ 65 GPa). At 69 GPa the sample is completely opaque. Threshold energy (E_{th}) is determined as the energy where optical density is 0.10. Above 50 GPa the optical density increases below the photon energy 1 eV (56 and 69 GPa). E_{th}'s above 50 GPa are obtained from the extrapolated curves (dashed curves).

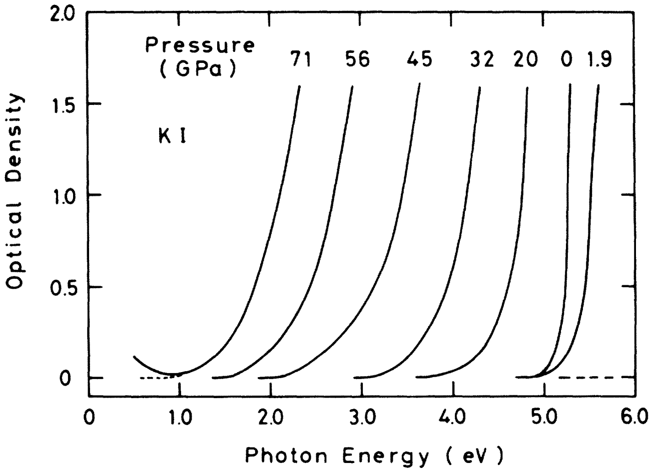

FIG. 3. Typical optical-density curves of KI at various high pressures. Above 40 GPa the optical absorption edge crosses over the visible region, so that the sample shows the continuous change in color from light yellow (~40 GPa) to orange (~71 GPa). Threshold energy ($E_{\rm th}$) is determined as the energy where the optical density is 0.10.

GPa. Figure 2 shows that the optical densities of RbI above 55 GPa increase below the photon energy 1 eV. The possible origins of this increasing will be mentioned later. The dashed curves at 56 and 69 GPa are extrapolated by assuming a similar form of that at 46 GPa. The dashed curve of KI at 71 GPa in Fig. 3 is similarly obtained. Figure 4 shows the threshold energies ($E_{\rm th}$) of optical absorption for RbI and KI as a function of pressure from 0 to 6 GPa obtained by using sapphire anvils. Here $E_{\rm th}$ was determined as the energy where the optical density is 0.10. Since the sample thickness at very high pressure is estimated to be 20~30 μm, the absolute value of the absorption coefficient at 0.10 optical density corresponds to $\sim 10^2$ cm^{-1}. As shown in Fig. 4, $E_{\rm th}$'s first increased with increasing pressure up to the $B1$-$B2$ phase-transition pressures (0.4 GPa for RbI and 1.9 GPa for KI), where they dropped rapidly. Above the pressures of phase transition they increased again and formed peaks at 2.5 GPa for RbI, and at 3.5 GPa for KI then they decreased monotonically with increasing pressure. The $E_{\rm th}$'s of RbI and KI at very high pressure are shown in Fig. 5. Above ~5 GPa the threshold energies decreased monotonically with increasing pressure. Here $E_{\rm th}$'s of RbI above 50 GPa were obtained from the extrapolated (dashed) curves in Fig. 2.

The relative volumes of RbI and KI obtained by the present high-pressure x-ray-diffraction study are shown in Fig. 6. Both materials showed discontinuous volume change at the $B1$-$B2$ phase transition. The relative volumes of $B2$-phase RbI and KI just after the transition were 0.84 and 0.80 for RbI and KI, respectively. Hereafter, these volumes are referred to as V_0^*: $V_0^* = 0.84V_0$ for RbI and $V_0^* = 0.80V_0$ for KI. After the $B1$-$B2$ transition, no structural transition was observed in the present x-ray-diffraction study. The CsCl-type crystal structure was found to be stable from 0.4 to 65 GPa for RbI and from 1.9 to 67 GPa for KI. The equation of state of second-order Birch-Murnaghan (BM) type was fitted to the P-V relations of RbI and KI in CsCl structure. The relationship is

$$P^* = \frac{3}{2}B_0\left[\left(\frac{V_0^*}{V}\right)^{7/3} - \left(\frac{V_0^*}{V}\right)^{5/3}\right] \times \left\{1+\frac{3}{4}(B_0'-4)\left[\left(\frac{V_0^*}{V}\right)^{2/3}-1\right]\right\}$$

where B_0 is the initial value of isothermal bulk modulus and B_0' is its pressure derivative. It should be noted here that P^* and V_0^* refer to the CsCl-type phase; P^* represents P-$P_{\rm tr}$, where $P_{\rm tr}$ is 0.4 and 1.9 GPa for RbI and KI, respectively, and "tr" refers to a transition. Bulk moduli and their pressure derivatives obtained from the least-squares fit to the second-order BM equations of state gives that $B_0 = 16.0 \pm 0.6$ GPa, $B_0' = 4.60 \pm 0.11$ for RbI, and $B_0 = 24.2 \pm 0.5$ GPa, $B_0' = 4.31 \pm 0.06$ for KI.

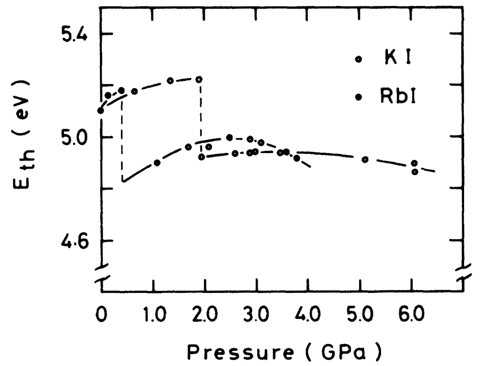

FIG. 4. Pressure dependence of the threshold energy below 6 GPa. $E_{\rm th}$ first increases with increasing pressure up to the $B1$-$B2$ transition pressure of 0.4 GPa (RbI) and 1.9 GPa (KI). At these pressures, $E_{\rm th}$ shows sudden decrease. After the transition $E_{\rm th}$ again increases, making peaks at 2.5 GPa (RbI) and 3.5 GPa (KI). Then it decreases monotonically.

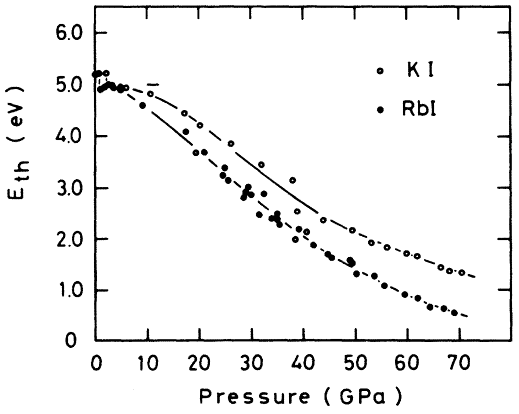

FIG. 5. Pressure dependence of the threshold energy at very high pressures. Above ~5 GPa $E_{\rm th}$ decreases monotonically with increasing pressure.

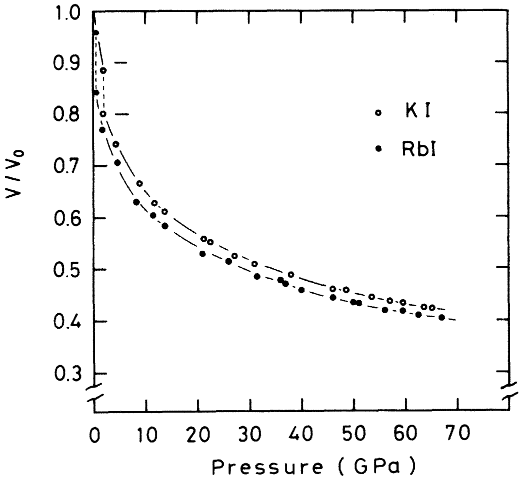

FIG. 6. Pressure-volume relations obtained by high-pressure x-ray-diffraction study. The solid and open circles represent the relative volumes of RbI and KI, respectively. Both materials exhibit the $B1$-$B2$ transition at 0.4 GPa (RbI) and 1.9 GPa (KI) accompanied with distinct volume decrease. For both materials the $B2$ structure is found to be stable up to the maximum pressure of the present study. The equations of state of the second-order Birch-Murnaghan type was fitted to P-V relations of RbI and KI both only for the $B2$ phase. Initial bulk moduli B_0 and its pressure derivatives B_0' are as follows: $B_0=16.0\pm0.6$ GPa, $B_0'=4.60\pm0.11$ for RbI, and $B_0=24.2\pm0.5$ GPa, $B_0'=4.31\pm0.06$ for KI. The solid lines correspond to least-squares fits to the data points.

IV. DISCUSSION

Ultraviolet absorption spectra of RbI and KI at 0 GPa have been obtained by Eby *et al.* (80 and 300 K (Ref. 5) and later by Teegarden and Baldini (10 K).[6] Band gaps of RbI and KI are found to increase as the temperature decreases (volumes decreases). This is consistent with the present study in a few GPa. Band gap of RbI and KI is 6.1 and 6.2 eV, respectively, at 80 K and it is about 6.0 eV at 300 K for both.[5] Below the band gap, a sharp absorption peak due to an exciton is observed at about 5.6 eV for both RbI and KI. The ultraviolet absorption by this exciton begins from about 5.1 eV.[5]

In this study, the onset of the sharp absorption was observed from 5.1 eV at 0 GPa for both RbI and KI as shown in Figs. 2–4. This onset corresponds to the threshold energy. Band-gap energy of RbI and KI is considered to be about 1 eV higher than this threshold energy and to increase as the absorption edge shifts as in Fig. 4. As mentioned previously the increase of this band-gap energy is consistent with that when temperature is lowered.

Although there is no evidence on the band-gap characters of RbI and KI after phase transition (in $B2$ phase) we may tentatively assume it to be a direct gap on analogy of CsI (Ref. 11); CsI has CsCl-type structure and a direct band gap at 0 GPa. At 2.5 GPa (RbI) and 3.5 GPa (KI) the threshold energy makes a peak, so that some changes are considered to take place in the band-gap character. Onodera *et al.*[12] calculated energy bands of KI at 0 GPa. According to their calculation, both the top of the valence band and the bottom of the conduction band are located at point $\vec{k}=0$ and the d bands which originate from the atomic $3d$ states of K^+ ions lie just above the lowest s-like conduction band. Although this calculation assumes NaCl-type structure, we consider that the characteristic is not so much affected by the $B1$-$B2$ transition. Then, the s-d band crossing is a possible origin of the peak of the threshold energy at 2.5 (RbI) and 3.5 GPa (KI). By assuming that the band-gap nature is direct also in the very high pressure region, the threshold energy shown in Fig. 5 gives the onset energy of exciton absorption. Because band gaps of RbI and KI at ambient conditions are almost the same (6 eV) and the threshold energies of optical absorptions are 5.1 eV for both, we may assume that the ratio of E_g to $E_{\rm th}$ is always constant, namely

$$\frac{E_g(p)}{E_{\rm th}(p)}=\frac{E_g(0)}{E_{\rm th}(0)}=1.20 .$$

By using this assumption, the band-gap (E_g) and threshold energies ($E_{\rm th}$) are plotted against the relative volume for the $B2$ phase of RbI and KI in Fig. 7. As shown in Fig. 7, E_g's of RbI and KI almost coincide if they were plotted against the relative volume in $B2$ structure. From Fig. 7 we can estimate the critical volumes of metallization to be 0.45 for both RbI and KI. This corresponds to critical pressures of 85 and 115 GPa for RbI and KI by the use of the equations of state mentioned previously. There still remains another possibility that the band-gap character is altered from direct to indirect at the $B1$-$B2$ transition or at the peak of $E_{\rm th}$. In this case $E_{\rm th}$ observed in the present study represents the band-gap energy. Thus,

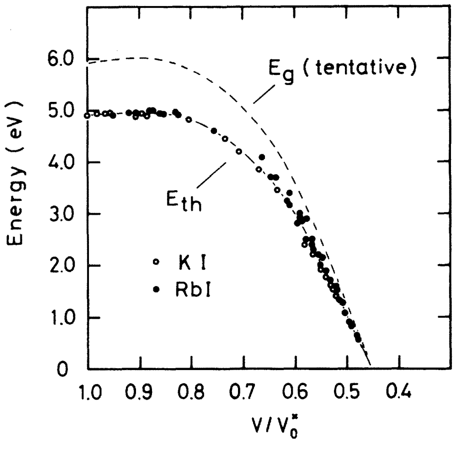

FIG. 7. Threshold energy ($E_{\rm th}$) as a function of the volume ratio in the $B2$ phase. Here, V_0^* represents the initial volumes of the $B2$ phase just after $B1$-$B2$ transition. $E_{\rm th}$'s of RbI and KI agree fairly well with each other when they are plotted as a function of relative volume in the $B2$ structure. Tentative band-gap energy (E_g) is shown by dashed curve which is obtained by assuming that the ratio of E_g to $E_{\rm th}$ is kept constant. Pressure-induced metallization may take place when the samples are compressed to $V=0.45V_0^*=0.38V_0$ for RbI and $V=0.45V_0^*=0.36V_0$ for KI. The corresponding pressures are determined to be 85 and 115 GPa for RbI and KI, respectively.

the quantitative results and conclusions as to metallization volumes and pressures remain unchanged.

Now we discuss the shapes of the optical-density curves shown in Figs. 2 and 3. As shown in these figures, the optical-density curves at high pressures increase more gradually than those at low pressures. This slow increase might be due to the pressure distribution within the sample: A typical sample diameter is about 50 μm at very high pressure which is one tenth of that of diamond-anvil faces. The pressure distribution amounts to $\pm 3\%$ at very high pressure. That slow increase might also be due to the fact that the pressures are not purely hydrostatic. As there is no medium which transmits purely hydrostatic pressure in half-megabar region, no pressure medium was employed in the present study. So the samples are considered to be in some stressed field. This can cause the broadenings of the electronic energy levels of RbI and KI. In fact a systematic discrepancy in lattice constants was observed in the present high-pressure x-ray-diffraction study. For example, the lattice constant obtained by (100) diffraction lines yielded large values by about 0.8% compared to that obtained by (110) lines for RbI at 67 GPa. Details of this systematic discrepancy in lattice constants will be published elsewhere.

As shown in Fig. 2 the absorption coefficient of RbI below the photon energy 1 eV increases rapidly as pressures increases. This increase in near ir region is possibly due to the absorption by phonons and their overtones. Excitation of free carriers is also a candidate of this origin, since the RbI above 50 GPa is considered to be a semiconductor from the viewpoint of its small energy gap: A similar increase of optical density of KI below 1 eV is observed as shown in Fig. 3 ($P=71$ GPa).

V. CONCLUSION

The pressure dependence of the fundamental optical absorption edges in RbI and KI crystals has been investigated up to 70 GPa with the aim at metallization. The x-ray-diffraction study has also been performed to confirm the crystal structure and to obtain the equations of state. After the $B1$-$B2$ phase transition at 0.4 and 1.9 GPa for RbI and KI, respectively, no structural transition was observed up to 67 GPa. The P-V relations in the $B2$ (CsCl) phase well fit to the equations of state of the second-order Birch-Murnaghan type. The metallization volumes (V_m) are estimated as follows:

$$V_m = 0.45 V_0^* = 0.38 V_0 \quad \text{for RbI}$$

and

$$V_m = 0.45 V_0^* = 0.36 V_0 \quad \text{for KI} .$$

Here V_0^* and V_0 are the initial volumes of CsCl- and NaCl-type structures, respectively. The corresponding metallization pressures of RbI and KI are estimated to be 85 and 115 GPa, respectively.

ACKNOWLEDGMENTS

The authors are grateful to Professor H. Kanzaki for providing facilities in optical absorption measurements and to Professor S. Akimoto and Dr. T. Yagi for providing the opportunity of x-ray-diffraction study. Thanks are also due to Professor T. Yamaguchi of Shizuoka University for helpful comments on the manuscript.

---

[1] See, for example, M. Ross and A. K. McMahan, in *Physics of Solid under Pressure,* edited by J. S. Schilling and N. R. Shelton (North-Holland, Amsterdam, 1981), p. 161, and references therein.

[2] Y. Kondo and K. Asaumi (unpublished).

[3] K. Asaumi and Y. Kondo, Solid State Commun. 40, 715 (1981).

[4] K. Asaumi, T. Mori, and Y. Kondo, Phys. Rev. Lett. 49, 837 (1982).

[5] J. E. Eby, K. J. Teegarden, and D. B. Dutton, Phys. Rev. 116, 1099 (1959).

[6] K. Teegarden and G. Baldini, Phys. Rev. 155, 896 (1967).

[7] See, for example, A. J. Cohen and R. G. Gordon, Phys. Rev. B 12, 3228 (1975), and references therein.

[8] H. K. Mao and P. M. Bell, Carnegie Inst. Washington Yearb. 77, 904 (1978).

[9] G. J. Piermarini, S. Block, J. D. Barnett, and R. A. Forman, J. Appl. Phys. 46, 2774 (1975).

[10] H. K. Mao, and P. M. Bell, J. W. Shaner, and D. J. Steinberg, J. Appl. Phys. 49, 3276 (1978).

[11] Y. Onodera, J. Phys. Soc. Jpn. 25, 469 (1968).

[12] Y. Onodera, M. Okazaki, and T. Inui, J. Phys. Soc. Jpn. 21, 2229 (1966).